

- Mandel, N., Mandel, G., Trus, B. L., Rosenberg, J., Carlson, G., & Dickerson, R. E. (1977) *J. Biol. Chem.* 252, 4619.
- Nall, B. T. (1983) *Biochemistry* 22, 1423.
- Nall, B. T. (1986) *Biochemistry* 25, 2974.
- Nall, B. T., & Landers, T. A. (1981) *Biochemistry* 20, 5403.
- Nall, B. T., Garel, J.-R., & Baldwin, R. L. (1978) *J. Mol. Biol.* 118, 317.
- Nall, B. T., Osterhout, J. J., Jr., & Ramdas, L. (1988) *Biochemistry* 27, 7310-7314.
- Osterhout, J. J., Jr., & Nall, B. T. (1985) *Biochemistry* 24, 7999.
- Osterhout, J. J., Jr., Muthukrishnan, K., & Nall, B. T. (1985) *Biochemistry* 24, 6680.
- Poerio, E., Parr, G. R., & Taniuchi, H. (1986) *J. Biol. Chem.* 261, 10976.
- Ramdas, L. (1987) Ph.D. Thesis, University of Texas Health Science Center, Houston, TX.
- Ramdas, L., & Nall, B. T. (1986) *Biochemistry* 25, 6959.
- Ramdas, L., Sherman, F., & Nall, B. T. (1986) *Biochemistry* 25, 6952.
- Schellman, J. A. (1978) *Biopolymers* 17, 1305.
- Schmid, F. X. (1982) *Eur. J. Biochem.* 128, 77.
- Schmid, F. X., & Baldwin, R. L. (1978) *Proc. Natl. Acad. Sci. U.S.A.* 75, 4764.
- Schmid, F. X., & Baldwin, R. L. (1979) *J. Mol. Biol.* 133, 285.
- Swanson, R., Trus, B. L., Mandel, N., Mandel, G., Kallai, O. B., & Dickerson, R. E. (1977) *J. Biol. Chem.* 252, 759.
- Takano, T., & Dickerson, R. E. (1981a) *J. Mol. Biol.* 153, 79.
- Takano, T., & Dickerson, R. E. (1981b) *J. Mol. Biol.* 153, 95.
- Takano, T., Trus, B. L., Mandel, N., Mandel, G., Kallai, O., Swanson, R., & Dickerson, R. E. (1977) *J. Biol. Chem.* 252, 776.
- Tanford, C. (1968) *Adv. Protein Chem.* 23, 121.
- Tsong, T. Y. (1974) *J. Biol. Chem.* 249, 1988.
- White, T. B., Berget, P. B., & Nall, B. T. (1987) *Biochemistry* 26, 4358.
- Wood, L. C., Muthukrishnan, K., White, T. B., Ramdas, L., & Nall, B. T. (1988) *Biochemistry* (preceding paper in this issue).
- Zuniga, E. H., & Nall, B. T. (1983) *Biochemistry* 22, 1430.

## Carbonyl $^{13}\text{C}$ NMR Spectrum of Basic Pancreatic Trypsin Inhibitor: Resonance Assignments by Selective Amide Hydrogen Isotope Labeling and Detection of Isotope Effects on $^{13}\text{C}$ Nuclear Shielding<sup>†</sup>

Erik Tüchsen\* and Poul Erik Hansen

*Institute of Life Sciences and Chemistry, University of Roskilde, P.O. Box 260, DK-4000 Roskilde, Denmark*

*Received March 23, 1988; Revised Manuscript Received August 16, 1988*

**ABSTRACT:** The carbonyl region of the natural abundance  $^{13}\text{C}$  nuclear magnetic resonance (NMR) spectrum of basic pancreatic trypsin inhibitor is examined, and 65 of the 66 expected signals are characterized at varying pH and temperature. Assignments are reported for over two-thirds of the signals, including those of all buried backbone amide groups with slow proton exchange and all side-chain carbonyl groups. This is the first extensively assigned carbonyl spectrum for any protein. A method for carbonyl resonance assignments utilizing amide proton exchange and isotope effects on nuclear shielding is described in detail. The assignments are made by establishing kinetic correlation between effects of amide proton exchange observed in the carbonyl  $^{13}\text{C}$  region with development of isotope effects and in the amide proton region with disappearance of preassigned resonances. Several aspects of protein structure and dynamics in solution may be investigated by carbonyl  $^{13}\text{C}$  NMR spectroscopy. Some effects of side-chain primary amide group hydrolysis are described. The main interest is on information about intramolecular hydrogen-bond energies and changes in the protein due to amino acid replacements by chemical modification or genetic engineering.

A variety of information about protein structure and dynamics in solution may be obtained from the carbonyl  $^{13}\text{C}$  NMR<sup>1</sup> spectrum (Gurd & Rothgeb, 1979; Kainosho et al., 1985b; Henry et al., 1987a,b). Of particular interest is the information inherent in this spectral region about the intramolecular hydrogen bonds that stabilize the backbone conformation. Knowledge about the stability and energy of these hydrogen bonds in the solution structure of the protein is essential for the understanding of protein folding, conforma-

tional dynamics, and hydrogen exchange.

The interest in the carbonyl region is boosted by recent reports on the deuterium isotope effects on  $^{13}\text{C}$  chemical shifts in model systems containing carbonyl and alcohol or amino groups (Reuben, 1986, 1987; Hansen, 1986). These model systems may be considered as remote analogues of amide groups in proteins. Large and variable deuterium isotope

<sup>†</sup> Supported by a grant from the Danish Natural Sciences Research Council.

<sup>1</sup> Abbreviations: NOE, nuclear Overhauser enhancement; NMR, nuclear magnetic resonance; BPTI, bovine pancreatic trypsin inhibitor; COSY, correlated spectroscopy; 2D, two dimensional; FID, free induction decay; TMS, tetramethylsilane; TSP, (tetramethylsilyl)propionate.

effects were found in molecules with a favorable geometry for intramolecular  $\text{C}=\text{O}\cdots\text{H}$  hydrogen bonds. The size of the deuterium effects over two covalent bonds,  $^2\Delta\text{C}=\text{O}(^2\text{H})$ , were found to be in the range 0.08–0.25 ppm and, interestingly, linearly correlated with the energy of the hydrogen bond (Reuben, 1986, 1987; Hansen, 1986). In non-hydrogen-bonded systems  $^2\Delta\text{C}=\text{O}(^2\text{H})$  is usually about 0.06 ppm, which is similar to the two-bond effect in amide model systems (Feeney et al., 1976; Hansen, 1983, 1987). Another parameter that holds information about the intramolecular  $\text{C}=\text{O}\cdots\text{H}-\text{N}$  hydrogen bonds is the chemical shift, which may be interpreted both for  $^{13}\text{C}$  carbonyl and for  $^1\text{H}$  amide resonances. Analyses of these are hampered by several contributing effects, some of which are poorly understood (Smith et al., 1987; Wagner et al., 1983; Llinas et al., 1977). Nevertheless, changes of the  $^{13}\text{C}$  carbonyl chemical shifts show a promise as a handle on changes caused by chemical modification or genetic manipulations.

To obtain valuable information about the protein on an atomic level, it is clearly a prerequisite that the spectral lines are assigned. For the BPTI  $^{13}\text{C}$  spectrum, regions other than the carbonyl region have now been assigned by cross-reference to the proton spectrum by proton-detected heteronuclear 2D NMR (Wagner & Brühwiler, 1986). This can be done for  $^{13}\text{C}$  atoms with directly bonded protons. So far, assignments of protein carbonyl resonances have heavily relied on selective  $^{13}\text{C}$  enrichment (Henry et al., 1987a,b; Kainosho et al., 1987, 1985a,b). This approach is restricted to microbial proteins, and the enrichment has been limited to selected amino acids. In small compounds, tertiary and carbonyl carbon resonances may be cross-referenced to vicinal proton resonances by methods utilizing the long-range couplings. Unfortunately, such methods are inapplicable to macromolecules with fast dipolar magnetic relaxation.

In the present paper we demonstrate how carbonyl resonances in the natural abundance  $^{13}\text{C}$  spectrum of BPTI can be resolved and assigned to the protein structure. We introduce an assignment method based on kinetic correlation of amide proton exchange with the development of the deuterium effect on the  $^{13}\text{C}$  carbonyl chemical shift. The proton exchange is measured by the disappearance of preassigned proton signals in the amide proton region. In the carbonyl region, the main emphasis is on the measurement of two-bond isotope effects between NH and CO within a given peptide group. For some residues we also observe large three-bond isotope effects which are helpful. These effects reach across the  $\alpha$ -carbon atoms. Additional information is obtained from analysis of pH titration shifts on the carbonyl resonances. The assignments of many of the resonances allow a systematic study of other effects influencing carbonyl chemical shifts. Treatment of BPTI for several days at low pH results in hydrolysis of one or more of the side-chain primary amide groups (Richarz et al., 1979). This process cannot easily be followed by  $^1\text{H}$  NMR, whereas the observation in the  $^{13}\text{C}$  carbonyl spectrum is straightforward.

## MATERIALS AND METHODS

BPTI was kindly provided by Novo Industries, Copenhagen, batch B2045-65-1. Deuterium oxide, 99.8%  $^2\text{H}$ , and deuter-

iated acids and bases were purchased from Aldrich Chemical Co. Other chemicals were of analytical grades or better. Values of pH are direct pH meter readings (Radiometer PHM26, equipped with an Ingold 6030-02 combination electrode) at 25 °C, calibrated with standard commercial buffers at pH 7.00 and 4.01.

Samples of BPTI for NMR spectroscopy contained 20–25 mM protein and 0.3 M KCl in a total volume of 0.5 mL. Adjustments of pH were performed by controlled addition of concentrated HCl or KOH from a microcapillary to the well-stirred protein solution while observing pH. Full  $^2\text{H}$  labeling of BPTI was obtained by heating solutions in  $^2\text{H}_2\text{O}$  at pH 3–4 to 90 °C for 5 min.

$^{13}\text{C}$  and  $^1\text{H}$  NMR spectra were measured at 63 and 250 MHz, respectively, in a Bruker AC250 spectrometer, equipped with a dual-tuned probe, allowing computer-controlled switching between the two spectral regions.  $^{13}\text{C}$  FID's were collected in 8K data blocks with the Bruker POWGATE pulse program. The spectra were collected at a narrow spectral width of 2500 Hz, centered in the carbonyl region. Proton noise decoupling was achieved with a relatively low decoupler power of ca. 1 W.  $^{13}\text{C}$  spectra were usually apodized by multiplication with a Gauss function and Fourier transformed into 16K data points.  $^1\text{H}$  spectra were either 2D magnitude COSY spectra or regular 1D spectra, according to the complexity of the  $^1\text{H}$  spectrum. Solvent presaturation was used in both cases. The 2D spectra were collected in  $128 \times 1024$  data matrices, and sine bell apodization was used in both dimensions. The spectra were zero filled to  $512 \times 1024$  data points on Fourier transformation. COSY spectra could be accumulated to a satisfactory signal/noise ratio in <45 min.

Spectral positions in the carbonyl region refer to a resonance at 170.0 ppm. The exact position of this peak relative to TMS is 169.96, and the chemical shift is pH independent over the range 1–7 (March et al., 1982). The position relative to TSP was found to be 172.48 ppm in a sample with the reference substance dissolved in the protein sample at pH 3.2. At an early stage the position of this peak was found to be unaffected by hydrogen isotope replacements. In the  $^1\text{H}$  region, the frequency scale was adjusted to the resolved Tyr-23  $\text{C}^*\text{H}_2$  doublet at 6.35 ppm.

Data sets for assignments by kinetic correlation consist of series of alternating  $^1\text{H}$  and  $^{13}\text{C}$  spectra for a sample with progressing exchange of a limited number of amide protons. Simplification of the amide proton spectrum was achieved by starting out with samples that are selectively proton labeled at a limited number of sites as previously described (Tüchsen & Woodward, 1985, 1987a–c; Tüchsen et al., 1987). Progression of the exchange is brought about outside the NMR probe by incubation in a water bath at a set temperature, by pH adjustments, or by short-term heating, or the sample is left exchanging in the NMR probe while the series of spectra are recorded. In the latter case, usually one-third of the  $^{13}\text{C}$  FID's are collected before the proton spectrum and then followed by the rest of the  $^{13}\text{C}$  spectrum in each cycle of the series. Thereby, comparable peak intensities are obtained in the two spectral regions.

The effect of amide  $^1\text{H}/^2\text{H}$  exchange on the carbonyl  $^{13}\text{C}$  and proton spectrum is outlined in Figure 1. Isotope effects from the peptide proton of a given residue,  $n$ , are expected both over two bonds on the adjacent carbonyl carbon (i.e.,  $\text{C}^\circ$  of residue  $n-1$ ) and over three bonds on  $\text{C}^\circ$  of the next peptide bond in the sequence (that is,  $\text{C}^\circ$  of residue  $n$ ). In case the amide proton of residue  $n$  is half-exchanged with  $^2\text{H}$  and the proton resonance has half of the original intensity, the  $^{13}\text{C}$

<sup>2</sup> The amino acid sequence of BPTI is Arg-1:Pro-2:Asp-3:Phe-4:Cys-5:Leu-6:Glu-7:Pro-8:Pro-9:Tyr-10:Thr-11:Gly-12:Pro-13:Cys-14:Lys-15:Ala-16:Arg-17:Ile-18:Ile-19:Arg-20:Tyr-21:Phe-22:Tyr-23:Asn-24:Ala-25:Lys-26:Ala-27:Gly-28:Leu-29:Cys-30:Gln-31:Thr-32:Phe-33:Val-34:Tyr-35:Gly-36:Gly-37:Cys-38:Arg-39:Ala-40:Lys-41:Arg-42:Asn-43:Asn-44:Phe-45:Lys-46:Ser-47:Ala-48:Glu-49:Asp-50:Cys-51:Met-52:Arg-53:Thr-54:Cys-55:Gly-56:Gly-57:Ala-58.

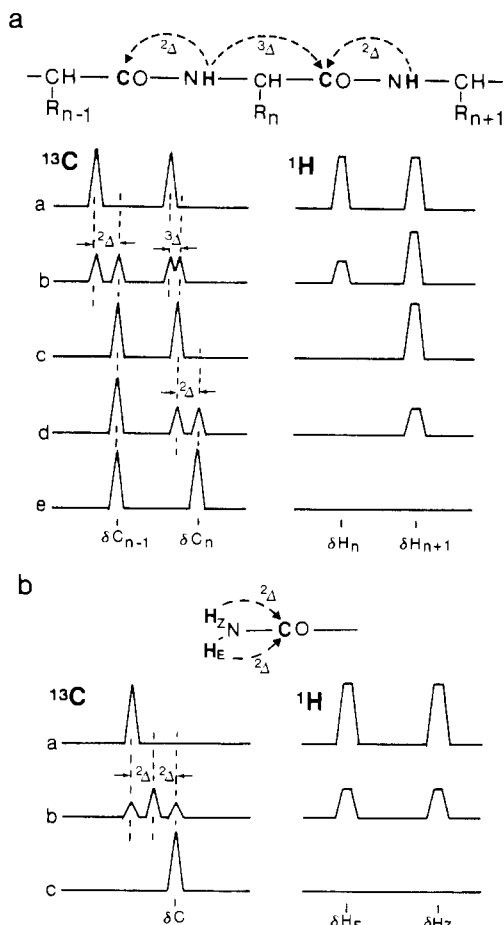


FIGURE 1: Effects of amide deuterium exchange in the amide  $^1\text{H}$  and carbonyl  $^{13}\text{C}$  regions of the NMR spectrum. (a) Backbone secondary amide groups. Trace a is for protein with  $^1\text{H}$ -labeled  $\text{NH}$ 's of residues  $n$  and  $n + 1$ . Traces b and c show the spectra after half-exchange and full exchange of residue  $n$ , and traces d and e show the spectra after subsequent half-exchange and full exchange of residue  $n + 1$ . (b) Primary amide groups. Traces a are for the fully  $^1\text{H}$ -labeled group, and b and c for half and the fully deuterium exchanged group, respectively. Independent exchange at equal rates is assumed for the primary amide protons.

resonances of residue  $n - 1$  is split into two halves with a distance,  $2\Delta$ , of approximately 0.08 ppm. Simultaneously, the  $^{13}\text{C}$  resonance of residue  $n$  may be split with a distance of  $3\Delta < 0.03$  ppm.

The primary amide carbonyl  $^{13}\text{C}$  chemical shift is subject to  $2\Delta$  effects from both amide protons, Figure 1b. Since the primary amide  $\text{NH}_2$  rotates (Tüchsen & Woodward, 1987b), the  $^1\text{H}$  intensities are always similar for the resonances of  $\text{H}_E$

and  $\text{H}_Z$ . The carbonyl resonance is split into three peaks with intensities proportional to the probabilities two, one, or zero  $^1\text{H}$  atoms bound to N. That is, assuming random exchange for one exchange half-life, the three peaks should have intensities of 0.25, 0.5, and 0.25, respectively, relative to the initial and final intensity.

## RESULTS AND DISCUSSION

**Carbonyl Spectrum.** The carbonyl region of the natural abundance  $^{13}\text{C}$  spectrum of small proteins such as BPTI may be resolved in standard medium field strength NMR spectrometers (Figure 2). BPTI contains 66 carbonyl carbon atoms in 57 peptide amide groups, 5 carboxylic groups (Asp-3 and -50, Glu-7 and -49, and Ala-58 C-terminus), and 4 side-chain primary amide groups (Asn-24, -43, and -44 and Gln-31). Positions of 65 carbonyl  $^{13}\text{C}$  resonances in BPTI are observed in Figure 2; 55 are fully resolved, 8 are in peaks of two resonances, and 3 resonances overlap in a single peak. The chemical shifts of the 65 observed resonances are listed in Table I at three values of pH across the carboxyl titration region. The clearness of the spectra is significantly better at  $\text{pH} < 3$ –4 than at pH values above the carboxyl titration region, where the resonance lines are somewhat broadened. This could be taken to indicate protein aggregation at  $\text{pH} > 4$ . However, line broadening is also observed for the solvent peak in the proton spectrum. Most likely, these effects are due to pH-dependent changes in the sample viscosity.

Many carbonyl resonances are heavily influenced by the carboxyl ionization equilibria (Figure 3), and relative resonance positions may be inverted by small changes in pH. The chemical shifts of the 65 resonances are listed at three pH values in Table I, and for other pHs relative positions may be obtained by reference to Figure 3. As it can be seen in Figure 3, most overlaps can be precluded by proper choice of pH. Carboxyl titration shifts are undetectable for only 11 of the 65 resonances in this pH region. Our data cannot fully account for the four to five resonances at 175.7–175.8 ppm at  $\text{pH} > 3$ , and the interpretation given in Figure 3 is tentative for these resonances. We suspect that the one lost resonance in the spectrum may be located in this region. A small peak appearing in Figure 2 at 175.5 ppm (labeled x) is absent in several other spectra obtained at varying pH. The peak at 177.8 ppm (Figure 2) is from an acetic acid impurity; it is greatly reduced or absent in spectra of samples which have been lyophilized at acidic pH.

**Kinetic Correlation for Peptide  $\text{C}=\text{O}$  Isotope Shifts.** Assignments of amide carbonyl  $^{13}\text{C}$  resonances by kinetic correlation of isotope effects and amide deuterium exchange, as outlined under Materials and Methods, rely on previous

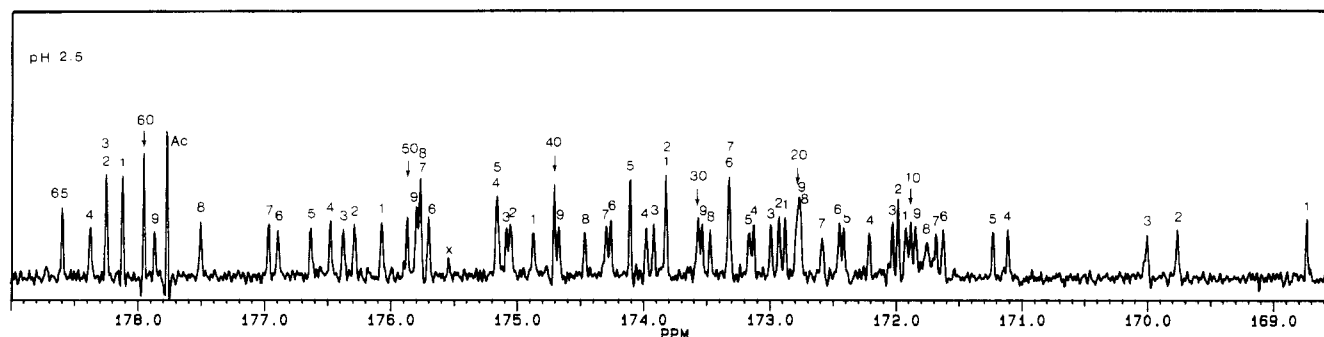


FIGURE 2: Carbonyl  $^{13}\text{C}$  spectrum of BPTI at 63 MHz. The sample contained 20 mM BPTI and 0.3 M KCl in  $^2\text{H}_2\text{O}$  at pH 2.5. Exchange equilibrium was attained by heating to 90  $^\circ\text{C}$  for 5 min, and the spectrum was acquired at 40  $^\circ\text{C}$ . 15 000 transients were collected over 9 h with low-power Waltz irradiation of the proton region. The summed FID was multiplied with a Gauss function and expanded from 8K to 16K data points before Fourier transformation. The frequency scale is adjusted to the resolved resonance at 170 ppm.

Table I: BPTI Carbonyl Spectrum

no.	chemical shift <sup>a</sup>			assignment <sup>b</sup>	no.	chemical shift <sup>a</sup>			assignment <sup>b</sup>
	pH 1.0	pH 3.0	pH 5.1			pH 1.0	pH 3.0	pH 5.1	
1	168.67	168.79	168.93	Arg-1 C <sup>o,c,d</sup>	34	173.96	173.98	174.10	(Pro-13 C <sup>o</sup> )
2	169.75	169.76	169.75	Phe-33 C <sup>o</sup>	35	173.49	174.89	176.99	Asp-50 C <sup>γ,c</sup>
3	170.00	170.00	170.00	Gly-12 C <sup>o,d,e</sup>	36	174.24	174.27	174.30	Asn-44 C <sup>γ,g</sup>
4	171.10	171.11	171.13	Phe-22 C <sup>o</sup>	37	174.29	174.30	174.25	
5	171.21	171.25	171.36	Cys-5 C <sup>o</sup>	38	174.44	174.48	174.54	(Thr-54 C <sup>o</sup> )
6	171.62	171.62	171.62	Gly-28 C <sup>o</sup>	39	174.67	174.66	174.62	Ile-19 C <sup>o</sup>
7	171.67	171.68	171.62	Arg-20 C <sup>o</sup>	40	174.39	175.20	177.69	Asp-3 C <sup>γ,c</sup>
8	171.74	171.75	171.73		41	174.90	174.82	174.68	Phe-45 C <sup>o</sup>
9	171.85	171.83	171.77		42	175.04	175.04	175.04	(Thr-11 C <sup>o</sup> )
10	171.87	171.89	171.90	Tyr-23 C <sup>o</sup>	43	174.90	175.32	176.02	Asp-50 C <sup>o</sup>
11	171.93	171.89	171.73	(Ser-47 C <sup>o</sup> )	44	175.14	175.20	175.37	Asn-44 C <sup>γ,g</sup>
12	172.13	171.79	171.32	Gly-57 C <sup>o,f</sup>	45	175.17	175.16	174.94	
13	172.02	172.02	171.98	Cys-30 C <sup>o</sup>	46	175.69	175.69	175.69	Lys-15 C <sup>o</sup>
14	172.21	172.19	172.15	(Cys-55 C <sup>o</sup> )	47	175.75	175.77	175.78	(Gly-37 C <sup>o</sup> )
15	172.42	172.39	172.35	Asn-44 C <sup>o</sup>	48	175.76	175.75	175.69	Asn-24 C <sup>γ,h</sup>
16	172.45	172.44	172.39	Gln-31 C <sup>o</sup>	49	175.80	175.78	175.76	
17	172.58	172.58	172.53		50	175.86	175.87	176.00	
18	172.75	172.76	172.93	Asn-43 C <sup>o</sup>	51	176.09	176.02	175.78	
19	172.76	172.76	172.77	Arg-17 C <sup>o</sup>	52	176.29	176.28	176.26	(Ala-27 C <sup>o</sup> )
20	172.78	172.78	172.80	Val-34 C <sup>o</sup>	53	176.35	176.39	176.43	Phe-4 C <sup>o</sup>
21	172.87	172.88	173.00	(Glu-7 C <sup>o,d</sup> )	54	176.47	176.48	176.52	(Leu-6 C <sup>o</sup> )
22	172.90	172.99	173.28	(Pro-8 C <sup>o,d</sup> )	55	176.60	176.68	177.29	(Glu-49 C <sup>o,f</sup> )
23	172.99	172.96	172.86	(Asn-24 C <sup>o</sup> )	56	176.89	176.89	176.88	(Ala-40 C <sup>o</sup> )
24	173.08	173.16	173.28		57	176.85	177.14	178.08	(Asp-3 C <sup>o,c,f</sup> )
25	173.15	173.16	173.17	Tyr-35 C <sup>o</sup>	58	177.50	177.50	177.53	
26	173.32	173.32	173.32		59	177.88	177.85	177.70	Ala-48 C <sup>o,f</sup>
27	173.32	173.32	173.37		60	177.76	178.27	181.91	Glu-49 C <sup>δ,c</sup>
28	173.44	173.50	173.62	Cys-51 C <sup>o</sup>	61	177.98	178.37	181.34	Glu-7 C <sup>δ,c</sup>
29	173.53	173.53	173.51		62	178.22	178.27	178.37	Met-52 C <sup>o</sup>
30	173.56	173.56	173.57	Thr-32 C <sup>o</sup>	63	177.47	179.17	180.70	Ala-58 C <sup>o,c</sup>
31	173.82	173.82	173.75		64	178.37	178.37	178.37	(Arg-53 C <sup>o</sup> )
32	173.82	173.82	173.79	Leu-29 C <sup>o</sup>	65	178.59	178.59	178.58	Gln-31 C <sup>δ,g,h</sup>
33	173.92	173.91	173.85	Tyr-21 C <sup>o</sup>					

<sup>a</sup> ppm for fully deuterated BPTI, 20–25 mM in <sup>2</sup>H<sub>2</sub>O, 0.3M KCl, 37 °C. Peak 3 fixed at 170.00 ppm. <sup>b</sup> Tentative assignments are in parentheses.

<sup>c</sup> Taken from March et al. (1982). <sup>d</sup> No isotope splitting in mixed <sup>1</sup>H/<sup>2</sup>H solvent. <sup>e</sup> Assignment supported by data of March et al. (1982)

<sup>f</sup> Assignment based on titration shift. <sup>g</sup> Primary amide isotope splitting observed. <sup>h</sup> Strongly affected by acid hydrolysis.

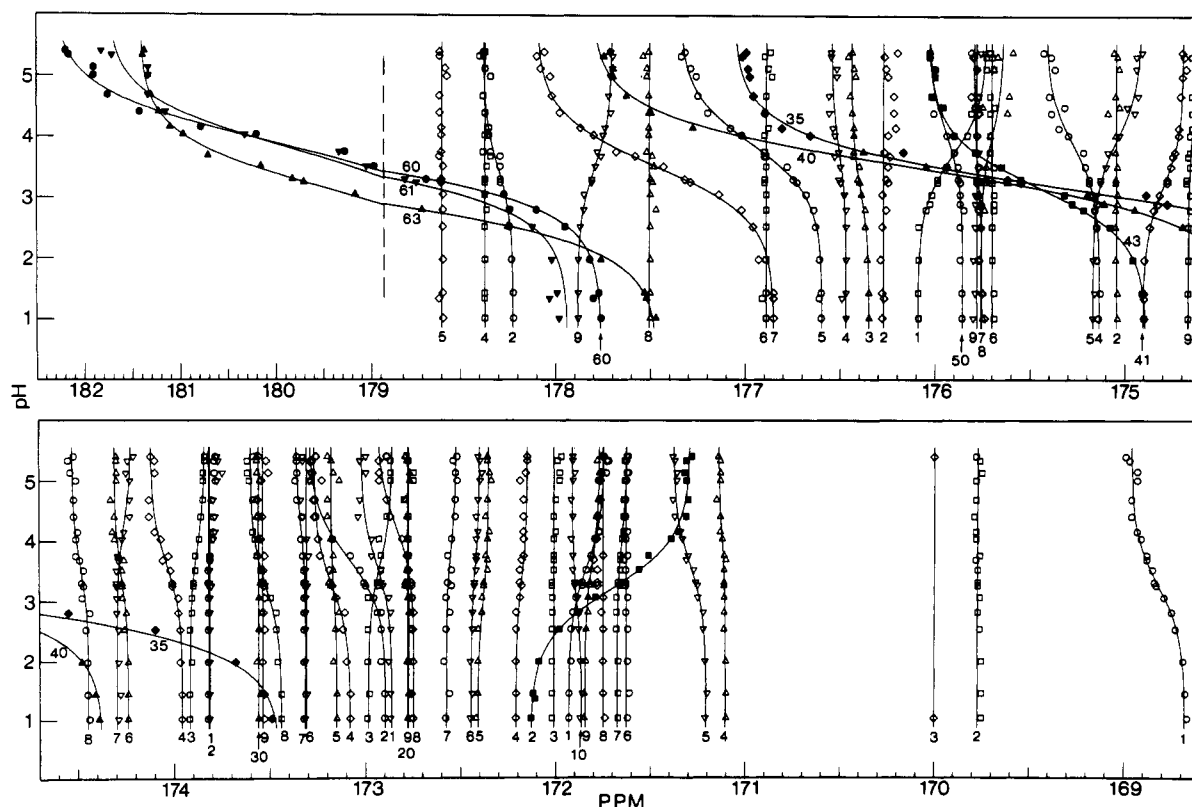


FIGURE 3: Chemical shift vs pH for the carbonyl spectrum of fully deuterated BPTI.

assignments of the amide <sup>1</sup>H resonances. Another prerequisite is that samples can be prepared for which only a limited

number of carbonyl group resonances show isotope splittings and that a simplified <sup>1</sup>H spectrum is at hand. A key method

Table II: Sample Preparations and Observed Proton Exchanges

preexchange in $^2\text{H}_2\text{O}$			Samples Starting from [ $^1\text{H}$ ]BPTI			
pH	time <sup>b</sup>	$t^c$	amide protons observed <sup>a</sup>			
11.0	1.0	25	Y21, F22, Y23			
9.0	1.0	25	I18, R20, Y21, F22, Y23, N24, Q31, Y33, Y32, F45			
8.5	0.5	25	I18, R20, Y21, F22, Y23, N24, L29, Q31, Y33, Y35, N44, F45			
1.3	10	37	(Y10), I18, R20, Y21, F22, Y23, N24, (L29), Q31, F33, Y35, (G36), N44, F45, C51, M52, R53, (C55)			
1.2	0.25	37	L6, G12, C14, C30, T32, C38, K41, T54			
0.5	5	37	I18, Y21, F22, Y23, N24, Q31, F33, (Y35), M52, R53, C55			
$^1\text{H}$ labeling			Samples Starting from [ $^2\text{H}$ ]BPTI			
pH	time <sup>b</sup>	$t^c$	pH	time <sup>b</sup>	$t^c$	amide protons observed
9.1	0.25	25	5.5	0.5h	40	I18, Y35, (G36)
9.3	1.0	25	8.8	0.5	20	I18, L29, Y35, N44, (N43s.c.)
1.0	3.0	40	8.6	0.5	5	N43s.c., (N24), (L29)
7.5	0.75	27	5.0	0.25	25	C5, L6, (E7), G36, G37, N44s.c., R53, C55
7.25	0.3	25	1.0	2.5	22	Y10, (G12), G28, V34, C38, T54, R53
5.7	0.25	20	1.0	0.5	21	C30, T32, V34
1.0	1.0	25	4.0	0.5	40	A16, N44s.c., (C51)
4.5	0.5	23	2.0	0.25	37	Y10, G12, A25, C30, T32, C38, A48, G56
3.0	0.5	23	1.0	0.25	37	K46, E49

<sup>a</sup> Low-intensity proton resonances are given in parentheses; s.c., side-chain primary amide protons. <sup>b</sup> Hours. <sup>c</sup> Degrees Celsius.

to obtain these conditions is the specific isotope labeling of the protein, by which a tailored  $^1\text{H}$  amide region is obtained.

An example of resonance assignments by kinetic correlation is shown in Figure 4. In this experiment, all but three exchangeable protons are first deuteriated at pH 11 (1 h at 25 °C). These are the NH's of Tyr-21, Phe-22, and Tyr-23, which are the slowest exchanging amide protons in BPTI. The carbonyl resonances of these peptide linkages ( $\text{C}^\circ$  of Arg-20, Tyr-21, and Phe-22, respectively) are pinpointed to resonances 4, 7, and 33, by observation of major differences relative to the spectrum of fully deuteriated BPTI (Figure 4). Differentiation within this group is obtained by further exchanging the protein at pH 11.4, 40 °C for 1 h. This results in almost full deuteriation of Tyr-21 and Tyr-23 NH, while Phe-22 NH remains fully  $^1\text{H}$  labeled. In the carbonyl spectrum, resonance 33 remains unaffected and is therefore assigned to  $\text{C}^\circ$  of Tyr-21. Resonance 4 is assigned to  $\text{C}^\circ$  of Phe-22 since a three-bond isotope effect is observed on deuteration of Phe-22 NH by heating the protein sample to 90 °C for 5 min. Resonance 7 is then assigned to  $\text{C}^\circ$  of Arg-20. This experiment illustrates the surprising observation that three-bond isotope effects are seen in some cases and not in others: A clear  $^3\Delta$  is observed from Phe-22 NH to Phe-22  $\text{C}^\circ$ , whereas no  $^3\Delta$  is observed for Tyr-21 or Tyr-23.

The assignments in Table I are based on several experiments in which samples are prepared with variable sets of  $^1\text{H}$ -labeled peptide linkages. Procedures for this NH tailoring are 2-fold. A variable portion of the exchangeable protons is exchanged with  $^2\text{H}$ , and effects of the remaining slowly exchanging protons are investigated. The composition and size of the sets are varied by choice of pH, exchange time, and temperature. Alternatively, the protein is first fully exchanged with deuterium and subsequently relabeled with  $^1\text{H}$  in variable sets of peptide linkages. It is our experience that the results become ambiguous when the proton region is overcrowded. Table II summarizes sample preparations and observed exchangeable protons in the experiments on which the assignments in Table I are based. Several specific assignments are obtained simply from the presence of an isotope effect in some experiments and not in others. For many resonances assignments can be narrowed to a few possible carbonyl groups. In some of these cases differentiation is obtained by careful comparison of the rates, while in others some ambiguity persists.

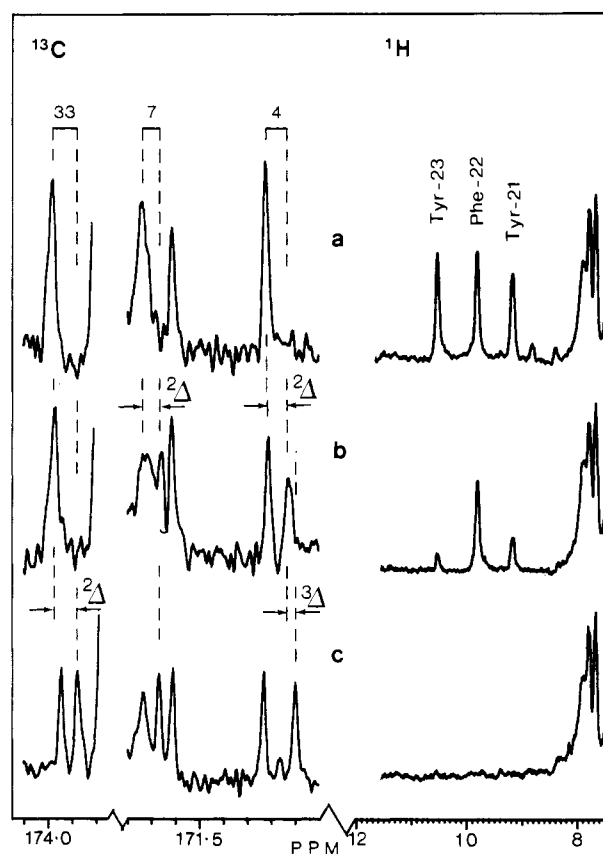


FIGURE 4: Assignment experiment for the carbonyl groups in the peptide linkages of the sequence Arg-20:Tyr-21:Phe-22:Tyr-23. Trace a shows the amide  $^1\text{H}$  region and segments of the carbonyl  $^{13}\text{C}$  region at pH 3.0 after exchange of all other amide protons (pH 11 for 1 h at 25 °C). Trace b is recorded after further exchange at pH 11.4, 40 °C, 1 h, and readjustment of pH to 3.0. Trace c shows the fully deuteriated protein spectrum, recorded after completion of the exchange by heating to 90 °C for 5 min.

In the present experiments we observe very slow acid-catalyzed exchange for several amide protons in the C-terminal helix. For example, after long-term exchange at pH 0.5, the amide protons of Cys-51, Met-52, Arg-53 are observed along with five of the  $\beta$ -core protons. For Arg-53 there is an apparent inconsistency with previously published data (Tüchsen

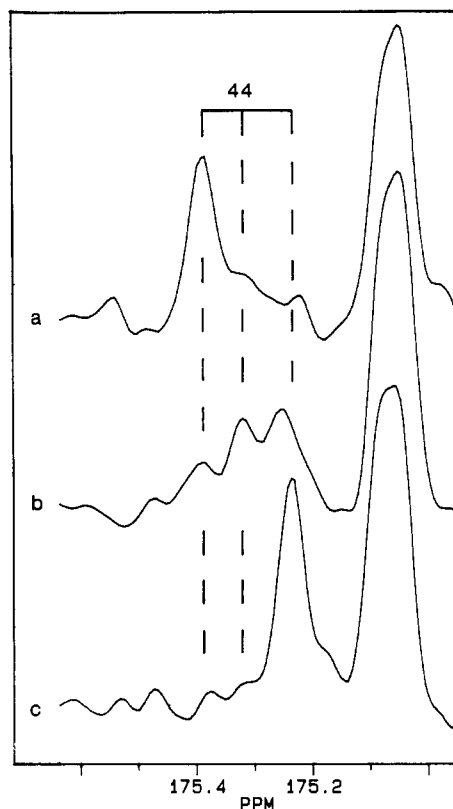


FIGURE 5: Assignment experiment for the primary amide carbonyl group of Asn-43. The protein sample contained 20 mM specifically  $^1\text{H}$ -labeled BPTI and 0.3 M KCl at pH 3.8, 40 °C (trace a). In trace b, Asn-43  $\text{N}^3\text{H}_2$  is ca. 50% deuteriated by short-term heating of the sample to 68 °C in a water bath. Spectrum c is recorded after completion of the exchange by heating the sample to 90 °C for 5 min.

& Woodward, 1987c), which indicated a relatively fast acid-catalyzed exchange for Arg-53 NH.

**Kinetic Correlation for Primary Amide C=O Isotope Shifts.** The special pattern for primary amide carbonyls associated with the exchange of the Asn-43 side-chain protons is observed for resonance 45 (Figure 5). At pH 3.8 of this experiment, resonance 45 is resolved from the other resonances in a gap in the spectra at 175.4–175.2 ppm. The upper and lower traces in Figure 5 show the peak positions for the fully  $^1\text{H}$ -labeled and fully  $^2\text{H}$ -labeled amide group, respectively. During the course of exchange, a peak transiently appears between the two positions, indicating amide groups with mixed label. The assignment to Asn-43 is unambiguous since no other primary amide groups exchange in this experiment. Resonance 36 was similarly assigned to the Asn-44 side chain in a specific proton labeling experiment (Table II).

The carbonyl  $^{13}\text{C}$  spectrum provides direct measure of the mechanism of primary amide proton exchange in the protein. Any cooperativity of the exchange may be evaluated from the variation of the three isotope peak intensities during the exchange. The sample used for trace b in Figure 5 had 60% of the Asn-43 primary amide protons exchanged for deuterium, as evaluated from the Asn-43  $\text{H}_\text{F}$  peak area in the proton spectrum (data not shown). For random and independent exchange of the two protons, relative peak intensities of 0.16, 0.48, and 0.36 are predicted for  $^1\text{H}_2$ ,  $^1\text{H}-^2\text{H}$ , and  $^2\text{H}_2$  species, respectively. In comparison, relative peak intensities in Figure 5 are 0.20, 0.38, and 0.42. That is, the fraction of protein mixed isotope label is smaller, and the fractions of protein with pure  $^1\text{H}$  or  $^2\text{H}$  are larger than expected for uncorrelated exchange, indicating a significant contribution of pairwise (correlated) exchange. This phenomenon is associated with

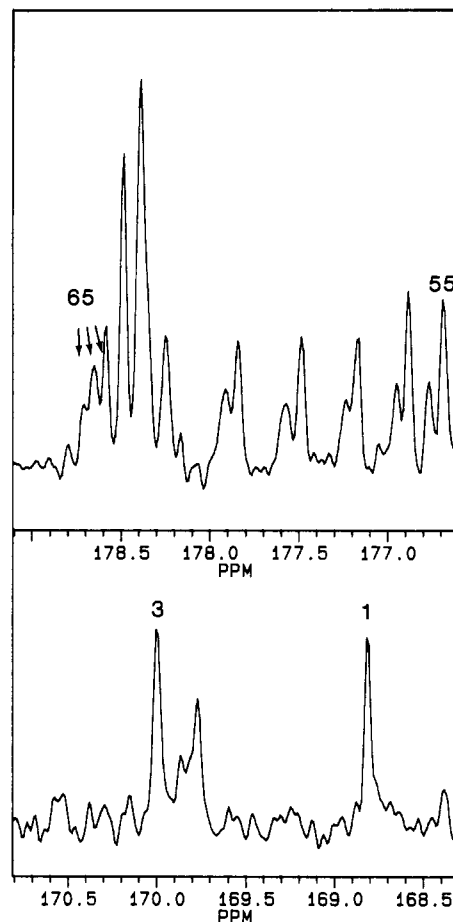


FIGURE 6: Segments of the  $^{13}\text{C}$  carbonyl spectrum of BPTI in water with mixed isotopes:  $^1\text{H}:^2\text{H} = 3:7$ ; pH 3.0; 40 °C; 0.3 M KCl. Amide solvent exchange was brought to equilibrium by heating the sample to 90 °C for 5 min.

the high activation energy mechanism of exchange which dominates at elevated temperatures (Woodward & Hilton, 1982). For measurements like these,  $^{13}\text{C}$  spectroscopy offers an advantage over a method based on NOE's in the  $^1\text{H}$  spectrum (Tüchsen & Woodward, 1987b; Roder et al., 1985) which may be influenced by magnetization transfer via  $\text{NH}_2$  group rotation and shifting relaxation mechanism with degree of exchange.

**Isotope Shifts in Mixed  $^1\text{H}/^2\text{H}$ -Labeled Water.** Carbonyl groups prior to proline residues in the sequence are expected to show no  $\Delta\text{C}=\text{O}(^2\text{H})$  and should be detectable in spectra obtained in mixed solvent or by comparison of spectra of the protein equilibrated in water of either isotope. Resonances 1 and 3 (Figure 6) obey this pattern. Resonance 1 was assigned to the peptide group of Arg-1-CON-Pro-2 (Richarz & Wüthrich, 1978). Resonance 3 responds to the titration of a tyrosine at pH ca. 10 (March et al., 1982) and may then be assigned to the Gly-12-CON-Pro-13 peptide group which is separated from the phenol oxygen of Tyr-10 by only 5.6 Å. The assignment of resonance 55 to Glu-7 C $^\alpha$  by March et al. (1982) is disproved by the clear isotope splitting seen in Figure 6.

The mixed solvent approach also allows the assignment of resonance 65 to a primary amide group, since this resonance splits into three components (Figure 6).

Equilibrium isotope effects in hydrogen exchange may be evaluated from the relative intensities of the components of the split peaks. Although an actual evaluation is not warranted from the experiment in Figure 6, it is interesting to notice that  $^1\text{H}:^2\text{H}$  ratios vary.

**pH Titration Shifts.** The variation of chemical shifts vs pH in Figure 3 reports changes in electrostatic environments of the carbonyl groups upon the ionization of the side-chain carboxylic groups. The curves drawn in Figure 3 are computed least-squares curves, assuming simple Brønsted titration behavior. For several residues the eye can easily detect small titration shifts, but our fitting program would not converge to a reasonable value of  $pK$ , and for these a line is drawn at the average chemical shift. A detailed analysis of the pH titration shifts is currently in progress.

The resonances of the five carboxylic carbonyls were previously assigned, on the basis of their very large titration shifts (Richarz & Wüthrich, 1976; March et al., 1984). For the two aspartic acid carbonyls, we cannot determine by inspection of the spectra whether they move parallelly or shift position relative to each other in the middle of the titration. The former interpretation is chosen since it provides a good match between  $pK$ 's computed for the carboxylic group and the assigned main-chain carbonyls. This interpretation is in agreement with both of the earlier reports. Unlike these, however, we see the two glutamic acid carboxyl resonances shift position during the titration. When the pH is raised from 1 to ca. 4, the distance between the two glutamic acid peaks gradually decreases, in a spectrum at pH 4.15 they overlap, and at higher pH they again come apart (Figure 3). As for the aspartic acid resonances the chosen interpretation gave the better match between  $pK$ 's calculated from the carboxylic resonances and assigned close by carbonyl resonances.

Titration shifts as shown in Figure 3 may corroborate assignments of carbonyl groups in the vicinity of carboxylic groups. In cases where kinetic correlation is ambiguous due to poorly distinguished exchange rates, the titration shifts provide means for discrimination. Many assignments were suggested by March et al. (1982) on the basis of the titration effects exclusively. In the present study we have confirmed the assignment of Asp-50 C $^{\alpha}$  to resonance 45 by observing the  $^2\Delta C=O(^2H)$  from Cys-51 NH. Some of their assignments are not confirmed in this study. The reason for this discrepancy is most likely that March et al. (1982), as mentioned above, rely exclusively on titration effects. The titration effect is not fully understood. Full account of the effect would require quantitative knowledge of the electrostatic effect originating from the carboxylate charges.

**Hydrolysis of Primary Amide Groups.** In an attempt to exchange the slowly exchanging amide protons, Tyr-21, Phe-22, and Tyr-23 the protein was treated at pH 1.3 or at pH 0.5 at 40 °C for several weeks. Exchange was achieved, but at the same time hydrolysis of the amide side chain of Asn-24 and Gln-31 occurred. This hydrolysis results in the disappearance of resonances 48 and 65 at 178.59 and 175.76 ppm and appearance of new resonances at 178.30 and 175.24 ppm. Though several other changes are observed as well, the general appearance of the spectrum is unchanged, indicating that the overall conformation of the protein is retained. At pH 0.5, the buried side-chain amide group of Asn-44 is also very slowly hydrolyzed, whereas the side chain of Asn-43 is unaffected.

The hydrolysis of the primary amide groups is not readily followed by means of  $^1H$  NMR, although new resonances have been reported upon prolonged heating of the protein at pH 3 (Richarz et al., 1979). One of these, appearing at 8.95 ppm, was also observed in this study. Other new  $^1H$  resonances appear at 8.68 and 6.42 ppm. The latter is a doublet lending its intensity from the Tyr-23 doublet at 6.35 ppm. These results are not fully understood, and further studies supported

by  $^{13}C$  NMR are needed.  $^{13}C$  NMR may prove useful not only in studies of primary amide hydrolysis but also in a more general sense in studies of the effects of amino acid replacements by genetic engineering.

**Temperature Effects.** The temperature effects are studied at pH 3 over the temperature range 25–50 °C. The majority of chemical shifts are largely constant over that interval. Large positive temperature shifts of 0.20 and 0.35 ppm are observed for the carboxyl carbonyls of Glu-7 (C $^{\delta}$ ) and the C-terminus, respectively. The positive sign means a shift to higher shielding (lower frequency) upon heating. For main-chain carbonyl carbons, temperature effects larger than 0.15 ppm are observed for Gly-57 C $^{\alpha}$  (0.24 ppm), Asp-3 C $^{\alpha}$  (0.26 ppm), and the unassigned resonances 58 and 48. Negative temperature effects are also observed, but the majority of the changes are positive.

The large effects observed for the C-terminus, Gly-57, and Asp-3 are in agreement with crystal studies (Wlodawer et al., 1984), in which it is clearly high mobility for both terminal strands outside the Cys-5...Cys-55 disulfide bridge. The large effect at Glu-7 C $^{\delta}$  is also expected as the side chain of this residue shows conformational heterogeneity and is ill defined in the crystal structure. It is likewise interesting to notice that Glu-49 C $^{\delta}$  shows only a moderate temperature effect. The side chain of this residue is hydrogen bonded to the backbone (Wlodawer et al., 1987). A change in temperature could perturb the hydrogen bonds, but no unusual effects are observed to support such a suggestion. The large effects can be explained simply by assuming that the temperature affects the rotamer populations of the side chains.

The temperature and the titration shifts are in general not found to be parallel, again supporting the conformational origin of the temperature effects.

**Analysis of Resonance Chemical Shifts.** The collection of assigned carbonyl shifts given in Table I provides a good opportunity to assess the usefulness of chemical shifts in assignments of protein carbonyl resonances. Several interesting features emerge. A carbonyl carbon in front of a proline residue becomes shifted 3 ppm to high field (lower frequency). An example is Gly-12 C $^{\alpha}$  resonating at 170.0 ppm, 3 ppm less than for C $^{\alpha}$  of glycines in the model peptides of Gurd et al. (1972). A similar shift can be deduced from the data of oxytocin (Walter et al., 1973), bradykinin (London et al., 1978), and smaller peptides (London et al., 1978; Urry et al., 1974), whereas Christl and Roberts (1972) report data for dipeptides showing effects of only 1 ppm. A high-field shift is also predicted by Torelli (1980). Another significant feature is a high-field shift for resonances of carbonyl groups involved in  $\beta$ -sheet structure. The effects are 1.5–5.5 ppm to higher field. A similar trend was observed by Kainosho et al. (1985a,b). Tyr-21 shows a slightly smaller effect. The broad variation is possibly due to effects of the side-chain conformation. It is unclear whether or not carbonyl resonances of the relatively short  $\alpha$ -helices show a characteristic chemical shift displacement.

A glance at Table I shows that the majority of unassigned resonances are in the central part of the carbonyl spectrum. These correspond to surface peptide groups with rapid NH exchange and not involved in rigid secondary structure. With the lack of hydrogen bonds to other than solvent, these carbonyl groups are expected to have chemical shifts similar to those of small peptides.

**Other Lines of Evidence.** Variable line shapes may be recognized for the peaks in Figure 2. The majority of the peaks have line widths of ca. 2 Hz (resolution enhancement omitted),

consistent with the overall molecular tumbling time and indicating no independent motion. Several resonances (e.g., 12, 35, 40, 61, and 62) are significantly sharper than most (line width ca. 1 Hz), indicating an added reorientation rate relative to the magnetic field. In spectra apodized with a Gaussian multiplication like Figure 2, these resonances appear with increased intensity. Indications of structural flexibility suggest assignments to side-chain carbonyl groups at the protein surface the peptide groups in the flexible termini of the main chain. The resonances from the side-chain carboxylic groups, as well as the C-terminal carboxyl and the main-chain carbonyl of Arg-1, have previously been assigned, on the basis of pH titration effects (Richarz & Wüthrich, 1978; Braun et al., 1978; March et al., 1982). Our data are consistent with theirs, and the side-chain carboxylic acid carbonyls of Asp-3, Asp-50, Glu-7, and Glu-49 are assigned to resonances 40, 35, 62, and 60, respectively, and the C-terminus Arg-1 is assigned to resonances 64 and 1 (Figures 2), respectively. Though the two termini constitute the most flexible parts of the backbone (Wlodawer et al., 1984), these resonances show no major difference in shape from other main-chain carbonyl resonances. March et al. (1982) suggested an assignment of resonance 12 to Gly-57 C $\alpha$ , and we agree that this is the most reasonable assignment. There is a perfect agreement with the titration shift of resonance 12 at pK ca. 3 and the short distance to either Asp-50 or the C-terminus. The side chains of Asn-43 and Asn-44 are in the rigid structure and were assigned above.

A few peaks, primarily resonances 8 and 17 (Figure 2), are broader and less intense than the majority. Peak 8 is split into two or more narrowly spaced peaks with unequal intensity, indicating conformational heterogeneity. Several side chains are indicated to have alternative and almost equally preferred conformations in the crystal form 2 and 3 structures (Wlodawer et al., 1984, 1987).

Other factors may influence the chemical shifts of specific resonances. These are the ionic strength and the temperature. It is essential to keep the concentration of KCl at such a level as to ensure constant ion strength.

## CONCLUSIONS

Several carbonyl resonances of the natural abundance  $^{13}\text{C}$  spectrum of BPTI have been assigned by establishing the kinetic correlation for amide hydrogen exchange as observed in the  $^1\text{H}$  spectrum by disappearance of NH resonances and in the  $^{13}\text{C}$  spectrum by development of isotope effects on the magnetic shielding. These include all main-chain carbonyl carbon resonances of the highly solvent-protected  $\beta$ -core. All carbonyl resonances connected to NH protons that exchange slowly on the time scale used to acquire a  $^{13}\text{C}$  spectrum can in principle be assigned by this method. The use of proteins with tailored amide  $^1\text{H}$  labeling is invaluable as it will be for most techniques which intend to correlate the  $^1\text{H}$  amide spectrum with resonances of the  $^{13}\text{C}$  spectrum.

An interesting and unexpected observation is the large variation of the three-bond isotope effect. A few three-bond effects were reported by Kainosho et al. (1987). Several are also observed in gramicidin S (Tüchsen and Hansen, unpublished results). An analysis of the isotope shifts in terms of molecular conformation is the topic of a forthcoming paper.

The very good resolution obtained of the BPTI carbonyl spectrum encourages investigations of other small-size proteins as well as larger proteins. Specific enrichments have shown that the resonances may be observed for proteins above the usual size limitation for NMR spectroscopy (Kainosho et al., 1985a,b). The high reproducibility of such spectra warrants the combined use of selective deuterium labeling and difference

spectroscopy, which can provide the necessary simplification of the spectra.

## SUPPLEMENTARY MATERIAL AVAILABLE

Full documentation for the assignments and isotope effects on the carbonyl spectrum from all the BPTI  $\beta$ -core protons (2 pages). Ordering information is given on any current masthead page.

**Registry No.** Basic pancreatic trypsin inhibitor, 9087-70-1.

## REFERENCES

- Brown, L. R., De Marco, A., Richarz, R., Wagner, G., & Wüthrich, K. (1978) *Eur. J. Biochem.* **88**, 87–95.
- Christl, M., & Roberts, J. D. (1972) *J. Am. Chem. Soc.* **94**, 4565–4573.
- Feeney, J., Partinton, P., & Roberts, G. C. K. (1976) *J. Magn. Reson.* **13**, 268–274.
- Gurd, F. R. N., & Rothgeb, T. M. (1979) *Adv. Protein Chem.* **33**, 73–165.
- Gurd, F. R. N., Keim, P., Glushko, V. G., Lawson, P. J., Marshall, R. C., Nigen, A. M., & Vigna, R. A. (1972) *Chemistry and Biology of Peptides*, Ann Arbor Science, Ann Arbor, MI.
- Hansen, P. E. (1983) *Annu. Rep. NMR Spectrosc.* **15**, 106–234.
- Hansen, P. E. (1986) *Magn. Reson. Chem.* **24**, 903–910.
- Hansen, P. E. (1988) *Prog. Nucl. Magn. Reson. Spectrosc.* **20**, 207–255.
- Henry, G. D., Weiner, J. H., & Sykes, B. D. (1987a) *Biochemistry* **26**, 3619–3626.
- Henry, G. D., Weiner, J. H., & Sykes, B. D. (1987b) *Biochemistry* **26**, 3619–3626.
- Henry, G. D., Weiner, J. H., & Sykes, B. D. (1987b) *Biochemistry* **26**, 3626–3634.
- Kainosho, M., Nagao, H., Uchida, K., Tomonaga, N., Nakamura, Y., & Tsuji, T. (1985a) *J. Mol. Struct.* **126**, 549–562.
- Kainosho, M., Nagao, H., Imamura, Y., Nakamura, Y., Tomonaga, N., Uchida, K., & Tsuji, T. (1985b) in *Magnetic Resonance in Biology and Medicine* (Govil, Khetrpal, & Saran, Eds.) Tata McGraw-Hill, New Delhi, India.
- Kainosho, M., Nagao, H., & Tsuji, T. (1987) *Biochemistry* **26**, 1068–1075.
- Llinas, M., Wilson, D. M., & Klein, M. P. (1977) *J. Am. Chem. Soc.* **99**, 6846–6850.
- London, R. E., Steward, J. M., Cann, J. R., & Matwiyoff, N. A. (1978) *Biochemistry* **17**, 2270–2283.
- Lyerla, J. R., Jr., & Freeman, M. H. (1972) *J. Biol. Chem.* **247**, 8183–8192.
- March, K. L., Maskalick, D. G., England, R. D., Friend, S. H., & Gurd, F. R. N. (1982) *Biochemistry* **21**, 5241–5251.
- Reuben, J. (1986) *J. Am. Chem. Soc.* **108**, 1735–1738.
- Reuben, J. (1987) *J. Am. Chem. Soc.* **109**, 316–321.
- Richarz, R., & Wüthrich, K. (1978) *Biochemistry* **17**, 2263–2269.
- Richarz, R., Sehr, P., Wagner, G., & Wüthrich, K. (1979) *J. Mol. Biol.* **130**, 19–30.
- Roder, H., Wagner, G., & Wüthrich, K. (1985) *Biochemistry* **24**, 7396–7407.
- Smith, G. M., Yu, L. P., & Domingues, D. J. (1987) *Biochemistry* **26**, 2202–2207.
- Torelli, A. E. (1980) *J. Am. Chem. Soc.* **102**, 7635–7637.
- Tüchsen, E., & Woodward, C. (1985) *J. Mol. Biol.* **185**, 405–419.
- Tüchsen, E., & Woodward, C. (1987a) *Biochemistry* **26**, 1918–1925.



- Tüchsen, E., & Woodward, C. (1987b) *Biochemistry* 26, 8073-8078.
- Tüchsen, E., & Woodward, C. (1987c) *J. Mol. Biol.* 193, 793-802.
- Tüchsen, E., Hayes, J. M., Ramaprasad, S., Copie, V., & Woodward, C. (1987) *Biochemistry* 26, 5163-5172.
- Urry, D. W., Mitchell, L. W., & Ohnishi, T. (1974) *Proc. Natl. Acad. Sci. U.S.A.* 71, 3265-3269.
- Wagner, G., & Brühwiler, D. (1986) *Biochemistry* 25, 5839-5843.
- Wagner, G., Pardi, A., & Wüthrich, K. (1983) *J. Am. Chem. Soc.* 105, 5948-5949.
- Walter, R., Prasad, K. U. M., Deslauries, R., & Smith, I. C. P. (1973) *Proc. Natl. Acad. Sci. U.S.A.* 70, 2086-2090.
- Wlodawer, A., Walter, J., Huber, R., & Sjölin, L. (1984) *J. Mol. Biol.* 180, 301-329.
- Wlodawer, A., Nachman, J., Gillard, G., Gallagher, W., & Woodward, C. (1987) *J. Mol. Biol.* 198, 469-480.
- Woodward, C. K., & Hilton, B. D. (1982) *Annu. Rev. Biophys. Bioeng.* 8, 99-127.

## CP4: A Pneumocyte-Derived Collagenous Surfactant-Associated Protein. Evidence for Heterogeneity of Collagenous Surfactant Proteins<sup>†</sup>

Anders Persson,<sup>‡</sup> Kevin Rust,<sup>‡</sup> Donald Chang,<sup>‡</sup> Michael Moxley,<sup>§</sup> William Longmore,<sup>§</sup> and Edmond Crouch<sup>\*‡</sup>

Department of Pathology, Jewish Hospital, Washington University School of Medicine, St. Louis, Missouri 63110, and Edward A. Doisy Department of Biochemistry, St. Louis University School of Medicine, St. Louis, Missouri 63104

Received March 28, 1988; Revised Manuscript Received June 13, 1988

**ABSTRACT:** Type II pneumocytes secrete pulmonary surfactant and are known to synthesize SP-35, a collagenous surfactant-associated protein. Freshly isolated type II cells also synthesize other bacterial collagenase-sensitive and hydroxyproline-containing proteins, including a glycoprotein designated CP4. CP4 was isolated from rat pneumocyte culture medium by immune precipitation with polyclonal antibodies to rat surfactant proteins or by DEAE chromatography and reverse-phase or gel permeation HPLC. CP4 did not cross-react with polyclonal antibodies to SP-35 and was completely resolved from SP-35 by SDS-PAGE ( $M_r$  43K reduced) or isoelectric focusing. Unlike SP-35, which consists of acidic isoforms assembled as disulfide-bonded dimers and multimers, CP4 was secreted as basic isoforms assembled as disulfide-bonded trimers. Differences in primary structure were demonstrated by CNBr and V8 protease peptide mapping. The secretion of both proteins was inhibited by 2,2'-dipyridyl, an inhibitor of posttranslational prolyl and lysyl hydroxylation and collagen triple helix formation. CP4 was isolated from EDTA extracts of rat surfactant. These studies provide evidence for the heterogeneity of pneumocyte-derived collagenous surfactant-associated proteins.

**P**ulmonary surfactant is comprised of specific phospholipids and several surfactant-associated proteins. The most abundant and best characterized of these proteins is designated SP-35 or SP-A. SP-35 has several distinctive structural features, including an amino-terminal collagenous domain, a central amphipathic domain believed to play a role in phospholipid binding, and a glycosylated carboxy-terminal domain that may mediate calcium-dependent carbohydrate binding (Benson et al., 1985; Floros et al., 1986b; Rannels et al., 1987; Sano et al., 1987; Ross et al., 1986). Surfactant also contains at least two different low molecular weight, noncollagenous, hydrophobic proteins (SP-18 and SP-5) (Claypool et al., 1984; Hawgood et al., 1987). There is evidence that these pneumocyte-derived proteins play important roles in modulating surface activity and in regulating the secretion and turnover of pulmonary surfactant (Dobbs et al., 1987; Hawgood et al., 1985, 1987; King et al., 1983; Wright et al., 1987).

We have observed that rat type II cells synthesize several collagenous components in primary culture. The major proline-labeled components secreted by adherent cells after 12-24 h in culture include type IV procollagen chains (CP1 and CP2)

and a low molecular weight collagenous protein (CP3) that does not cross-react with polyclonal antibodies to rat surfactant proteins (Crouch et al., 1987a). We have recently identified two additional pneumocyte-derived collagenous proteins (CP4 and CP5). These proteins are secreted by type II cells during the first day of primary culture and are immunologically related to proteins in normal rat surfactant. CP5 corresponds to SP-35. However, CP4 is immunologically and structurally different from SP-35, the previously described hydrophobic surfactant-associated proteins, and other low molecular weight collagenous proteins.

### MATERIALS AND METHODS

**Type II Cell Isolation.** Rat type II cells were isolated by limited modifications of the method of Dobbs et al. (1986). Briefly, adult male Sprague-Dawley rats were anesthetized, heparinized, tracheostomized, and sacrificed by exsanguination as previously described (Crouch et al., 1987a). The lungs were perfused via the pulmonary artery with phosphate-buffered saline (PBS) to remove blood and lavaged repeatedly via the trachea with divalent cation-free HEPES-buffered saline to obtain crude surfactant and to remove macrophages. Porcine pancreatic elastase (Elastin Products, Inc., Pacific, MO; 30 orcein units/mL) was instilled into the airway in three aliquots, each to total lung capacity, for a total of 20 min at 37 °C. The lungs were minced in the presence of 250 µg/mL DNase I (Boehringer-Mannheim), and elastase was inactivated by the

<sup>†</sup> This study was supported by Program Project Grant HL-29594 and NIH Training Grant 5-T32-HL07317.

<sup>\*</sup> Address correspondence to this author at the Department of Pathology, Jewish Hospital, 216 S. Kingshighway, St. Louis, MO 63110.

<sup>‡</sup> Washington University School of Medicine.

<sup>§</sup> St. Louis University School of Medicine.